

# An anatomically realistic voxel model of the pregnant woman and numerical dosimetry for a whole-body exposure to RF electromagnetic fields

T. Nagaoka<sup>1</sup>, T. Togashi<sup>2</sup>, K. Saito<sup>3</sup>, M. Takahashi<sup>3</sup>, K. Ito<sup>4</sup>,  
T. Ueda<sup>5</sup>, H. Osada<sup>6</sup>, H. Ito<sup>7</sup> and S. Watanabe<sup>1</sup>

<sup>1</sup>National Institute of Information and Communications Technology  
4-2-1 Nukuikita-machi, Koganei, Tokyo 184-8795, Japan

<sup>2</sup>Graduate School of Science and Technology, Chiba University  
1-33 Yayoi-cho, Inage-ku, Chiba 263-8522, Japan

<sup>3</sup>Research Center for Frontier Medical Engineering, Chiba University  
1-33 Yayoi-cho, Inage-ku, Chiba 263-8522, Japan

<sup>4</sup>Faculty of Engineering, Chiba University  
1-33 Yayoi-cho, Inage-ku, Chiba 263-8522, Japan

<sup>5</sup>Department of Radiology, Institute of Clinical Medicine, University of Tsukuba  
1-1-1 Tennodai, Tsukuba 305-8575, Japan

<sup>6</sup>Department of Obstetrics and Gynecology, Juntendo University Shizuoka Hospital  
1129 Nagaoka, Izunokuni 410-2295, Japan

<sup>7</sup>Radiation Oncology, Graduate School of Medicine, Chiba University  
1-8-1 Inohana, Chuo-ku, Chiba 260-8670, Japan

**Abstract**—The numerical dosimetry of pregnant women is one of the most important issues in electromagnetic-field safety. We have recently developed a whole-body numerical female model of an adult Japanese (non-pregnant) average figure. Therefore, a new fetus model including inherent tissues of pregnant women was constructed based on abdominal MRI data of a 7-month pregnant woman. A whole-body pregnant woman model was developed by combining the new fetus and the female models. The anatomical details of the developed pregnant woman model and basic SAR characteristics for whole-body exposure to RF electromagnetic fields are demonstrated.

## I. INTRODUCTION

There has been increasing concern about safety of human-body of radio-frequency (RF) electromagnetic field due to dissemination of wireless telecommunication devices. In addition, electric appliances operated at frequencies higher than the power frequency (e.g., an induction heater cooker), such as the intermediate frequency (IF), have raised new interest in their impact on health. Pregnant women may use these devices and electric appliances. Therefore, the dosimetry of pregnant women is one of the most important issues in electromagnetic-field safety. Because the internal electromagnetic field strength is difficult to be measured inside a human body, it is necessary to be estimated by numerical methods using voxel-based models, the anatomical structure of which is constructed as a set of minute elements (voxels).

New whole-body voxel models have been developed from magnetic resonance imaging (MRI), X-ray computed tomography, or anatomical color images of the Visible Human Project (VHP) [1]-[7]. These voxel models are adult male and female and child models. No whole-body voxel model for pregnant women has been developed, although some abdomen models have been done [8], [9]. Therefore, an anatomically realistic whole-body model needs to be developed for numerical analyses of pregnant women.

The purpose of this study was to develop a whole-body model of the pregnant woman. However, developing a new high-resolution model from medical imaging devices is very difficult because of ethical problems in obtaining whole-body tomographic images of a healthy subject. In addition, developing a new model requires a tremendous amount of time. Therefore, we only scanned the abdomen of a pregnant woman volunteer using MRI. A fetus model was constructed based on the newly acquired abdomen images. A pregnant woman model was developed by combining this new fetus voxel model with an existing whole-body voxel model of a non-pregnant female.

The next section describes the construction of the pregnant woman model. Section 3 outlines the characteristics of the developed pregnant woman model. A preliminary study for numerical dosimetry using the pregnant woman model is demonstrated in section 4.

## II. THE PREGNANT WOMAN MODEL

### A. Whole-body non-pregnant female model

The first high-resolution realistic whole-body voxel female model in Japan was developed by Nagaoka et al [7]. The National Institute of Information and Communications Technology in Japan distributes this model for nonprofit research purposes with free of charge. The details are described in the agreement document which can be found at the following URL ([http://emc.nict.go.jp/menu\\_E.html](http://emc.nict.go.jp/menu_E.html)). This voxel model is shown in Fig. 1. It was developed by collecting MRI data from a Japanese adult female who had average height and weight. This model is also in the upright position, as if the woman is standing on the ground with her hands at the sides of her body, and it is composed of  $2 \times 2 \times 2$  mm<sup>3</sup> voxels, and is segmented into 51 different tissues and organs. The body dimensions and internal organ masses of this model are close to the average Japanese values.

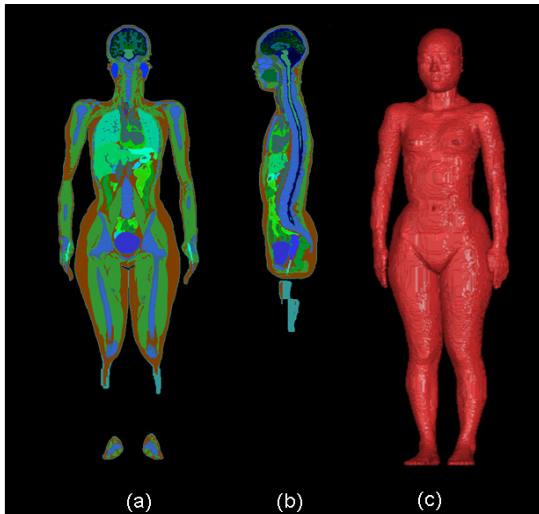


Fig. 1. Female model (non-pregnant). (a) Mid-coronal display. (b) Mid-sagittal display. (c) Surface display.

### B. Fetus model

Abdominal MR images of a 7-month pregnant woman volunteer were taken using a 1.5 T MRI machine. Each image had a slice thickness of 2 mm and a matrix size of  $512 \times 512$  with a 380 mm field-of-view (FOV). The transverse images were interpolated along the axial direction to yield an isotropic volume data set. A total of 361 transverse images of the abdomen were taken. The spatial-resolution of the images was  $0.742 \times 0.742 \times 0.742$  mm<sup>3</sup>.

Inherent tissues of pregnant women, including the fetus, were identified using image analysis software (SliceOmatic ver. 4.3; Tomovision Inc., Montreal). This software has powerful segmentation tools with a highly interactive interface. Figure 2 shows an example of an original MR image and a tissue-identified image. A three-dimensional abdominal image was constructed by combining the identified transverse images. Misidentifications were corrected by using this three-dimensional image and the three

orthogonal planes (axial, sagittal, and coronal). We also smoothed out the boundaries of tissues by checking the three-dimensional images and the three orthogonal planes.

Figure 3 shows the fetus model. This model is classified into 6 different types of tissues (fetus, fetal brain, fetal eyes, amniotic fluid, placenta, and uterus wall).

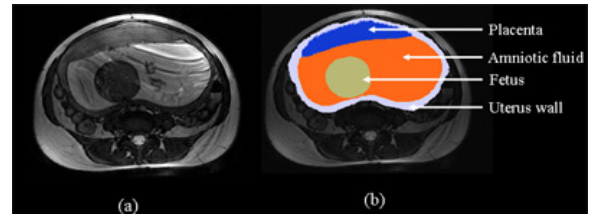


Fig. 2. Example of transverse images before and after identification of tissues. (a) Original MR image, (b) tissue-identified image at the same level.

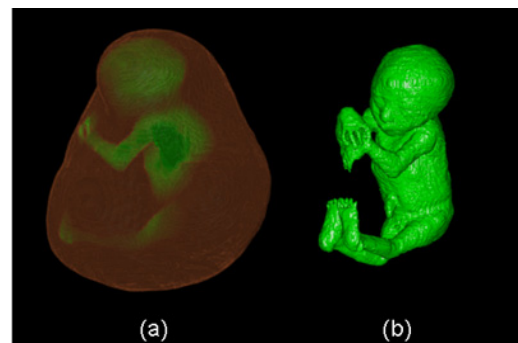


Fig. 3. Developed fetus model. (a) Volume rendering display. (b) Surface display of the fetus.

### C. Pregnant woman model

The pregnant woman model except of the fetus and its surrounding tissues was developed by deforming the non-pregnant adult woman model. The abdomen of the female model was dilated to match with the shape of the pregnant woman's abdomen.

We applied the free-form deformation (FFD) algorithm for abdominal deformation [10]. The FFD algorithm can globally transform the shape by moving the control points which defines the shape of the model as we want to transform. This technique does not limit the shape of the transformation because it uses the parameter space in the control cell and can keep the continuity of the object.

Skin, fat, and muscle were extracted from the non-pregnant model. These tissues were deformed for reference with the original MR images (abdomen) of the pregnant model. Figure 4 shows the change in the shape of the model abdomen.

These deformed tissues were combined with other non-deformed tissues and organs. The voxel size of the fetus model ( $0.742 \times 0.742 \times 0.742$  mm<sup>3</sup>) including amniotic fluid, placenta, and uterus wall was rescaled to  $2 \times 2 \times 2$  mm<sup>3</sup>. The fetus model was fitted in the abdomen of the deformed model. Then, thorough correction of the developed pregnant model was performed under the supervision of medical doctors.

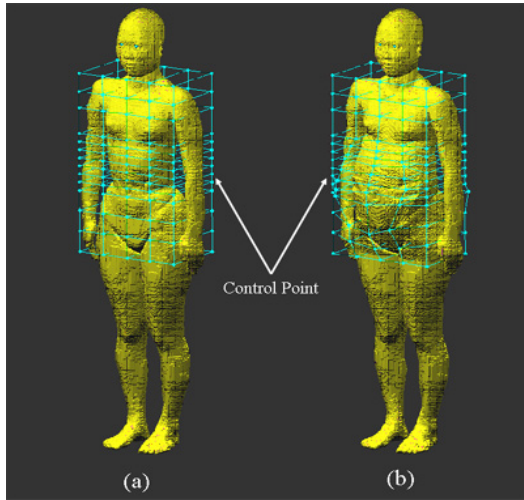


Fig. 4. Change in shape of abdomen. (a) Female model before deforming abdomen. (b) After deforming abdomen.

### III. CHARACTERISTICS OF THE PREGNANT WOMAN MODEL

Figure 5 shows the developed pregnant woman model. The model is segmented into 56 different tissues and organs.

The specific absorption rate (SAR), which is the amount of RF energy absorbed in the unit weight of the body, is used as a measure of the thermal effects of the RF electromagnetic-field exposure. It is known that SAR is influenced by various factors such as body size and position and size of the internal tissues. Therefore, the body dimensions for the abdomen of the developed pregnant woman model were compared with average Japanese values of 7-month pregnant women [11]. The measurement regions are shown in Fig. 6. The comparison results are shown in Table 1. In the pregnant model, all of the dimensions in front-to-back direction were smaller than those of the average values, while all of the dimensions in left-to-right direction were larger than those of the average values. The reason for

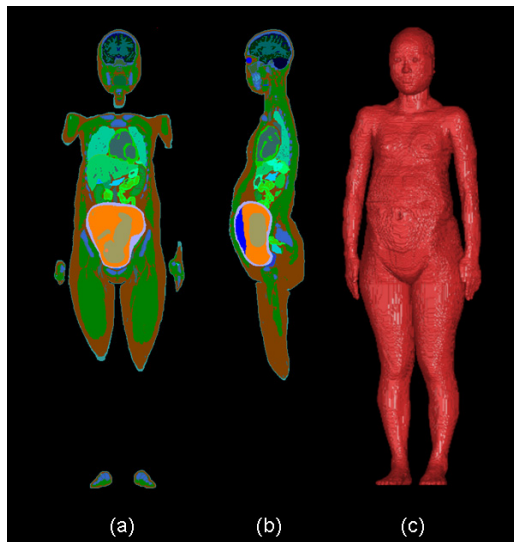


Fig. 5. 7-month pregnant woman model. (a) Mid-coronalal display. (b) Mid-sagittal display. (c) Surface display.

these differences is conceivably a difference in posture when measuring the body parts. The developed model was based on MRI data obtained in the dorsal position, whereas the average values were obtained in an upright position. Nevertheless, most of the dimensions around the lower abdomen including the fetus and it surrounding tissues were close to the average Japanese values.

Inherent tissues of the pregnant women were also compared with reference values [12], [13]. The results are shown in Table 2. These tissues in the pregnant model were close to the reference values except amniotic fluid.

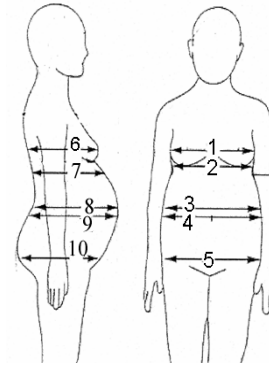


Fig. 6. Measured body dimensions.

Table 1  
Comparison of body dimensions between the pregnant woman model and the average Japanese references

Region number	Model (mm)	Average (mm)	Model-to-average ratio
1	296	290	1.02
2	272	257.4	1.06
3	326	303.9	1.07
4	304	280	1.09
5	380	336.8	1.13
6	188	249.3	0.75
7	190	236.6	0.80
8	226	243.7	0.93
9	244	263	0.93
10	224	252.7	0.89

### IV. NUMERICAL DOSIMETRY FOR PREGNANT WOMAN MODEL

#### A. Calculation method and model

The finite-difference time-domain (FDTD) method was used to evaluate internal electromagnetic fields of the pregnant model exposed to E-polarized plane waves (10 MHz to 2 GHz) propagating from the front to the back of the body.

The incident power density was  $1 \text{ mW/cm}^2$ , which was the reference level for occupational exposure to electromagnetic fields at the VHF band [14]. Perfectly matched layer (PML) boundary conditions (8 layers) [15] were assumed at all boundaries of the calculation region because the absorbing boundary was such that the pregnant woman model could be assumed to be in free space. The cell size of the calculation

Table 2  
Comparison of inherent tissues between the pregnant woman model and the reference values

	Fetus model	Reference value (50 percentile)	Model-to-reference value ratio
Fetal height (cm)	37.6	37.6	1.00
Fetal body weight (kg)	0.84	1.2	0.7
Fetal brain weight (g)	120	150	0.81
Amniotic fluid (ml)	2100	750	3.01
Placental weight (g)	387	400	0.97

region was  $2 \times 2 \times 2 \text{ mm}^3$ . The PML boundaries were set 100 cells apart from the nearest parts of the model. Electrical properties corresponding to the tissues were taken from different studies [16]-[19]. The electrical properties of tissues not described in these sources were substituted with electrical properties of other tissues described in these sources.

### B. SAR characteristics

The whole-body averaged SARs of pregnant woman and adult female (non-pregnant) models are shown in Fig. 7. The whole-body averaged SARs of both models become a maximum around the whole-body resonant frequency (80 MHz), and SAR values are very close to each other. These results suggest that pregnancy does not affect the whole-body averaged SAR.

SAR values averaged for inherent tissues of pregnant women are shown in Fig. 8. The SAR values are normalized by the whole-body average SAR corresponding to that in Fig. 7. The SARs of these inherent tissues were found to be less than or nearly equal to the whole-body averaged SAR.

## V. CONCLUSION

The fetus voxel model was constructed based on abdominal MRI data from the 7-month pregnant woman volunteer. The pregnant woman model was developed by combining the new developed fetus model and the deformed model based on the non-pregnant adult Japanese female model. The developed pregnant woman model consists of  $2 \times 2 \times 2 \text{ mm}^3$  voxels, and is segmented into 56 different tissues. Therefore, a highly precise simulation for pregnant women and/or the fetus is possible using this whole-body pregnant woman model. SAR estimation of the pregnant woman model exposed to E-polarized electromagnetic waves from 10 MHz to 2 GHz was demonstrated as an example of an application of this model. We plan to make data from the developed pregnant woman model available to the public for use in various research after further improvement processes.

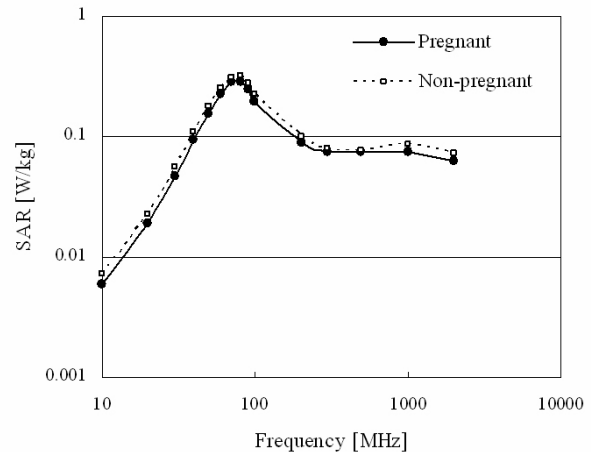


Fig. 7. Whole-body average SARs of pregnant women and non-pregnant female models exposed to E-polarized plane waves.

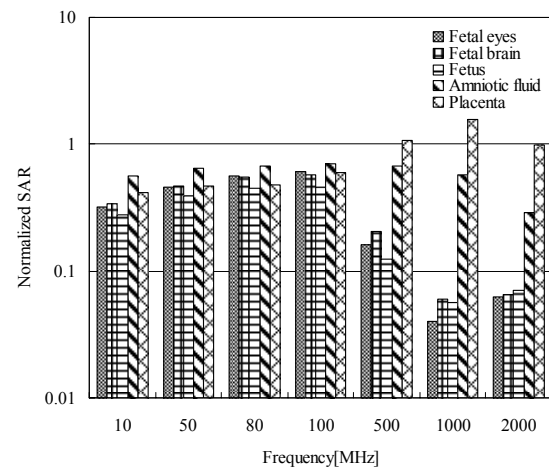


Fig. 8. Inherent tissues of SARs of pregnant women.

## REFERENCES

- [1] Dimbylow PJ, "FDTD calculations of the whole-body averaged SAR in an anatomically realistic voxel model of the human body from 1 MHz to 1 GHz," *Phys. Med. Biol.*, vol. 42, pp. 479-490, 1997.
- [2] Dimbylow PJ, "Development of the female voxel phantom, NAOMI and its application to calculations of induced current densities and electric fields from applied low frequency magnetic and electric fields," *Phys. Med. Biol.*, vol. 50, pp. 1047-1070, 2005
- [3] Gandhi OP, Furse CM, "Millimeter-resolution MRI-based models of the human body for electromagnetic dosimetry from ELF to microwave frequencies," *Proc. Int. Workshop on Voxel Phantom Development*, Chilton, UK: National Radiological Protection Board, 6-7 July, pp. 24-31, 1995.
- [4] Dawson TW, Caputa K, Stuchly MA, "A comparison of 60 Hz uniform magnetic and electric induction in the human body," *Phys. Med. Biol.*, vol. 42, pp. 2319-2329, 1997.
- [5] Gajsek P, Hurt WD, Ziriak JM, Mason PA, "Parametric dependence of SAR on permittivity values in a man model," *IEEE Trans. Biomed. Eng.*, vol. 48, pp. 1169-1177, 2001.
- [6] Sandrini L, Vaccari A, Malacarne C, Cristoforetti L, Pontalti R, "RF dosimetry: a comparison between power absorption of female and male numerical models from 0.1 to 4 GHz," *Phys. Med. Biol.*, vol. 49, pp. 5185-5201, 2004.
- [7] Nagaoka T, Watanabe S, Sakurai K, Kunieda E, Watanabe S, Taki M, Yamanaka Y, "Development of realistic high-resolution whole-body voxel models of Japanese adult and females of average height and weight, and application of models to radio-frequency

- electromagnetic-field dosimetry," *Phys. Med. Biol.*, vol. 49, pp. 1-15, 2004.
- [8] Kainz W, Chan DD, Casamento JP, Bassen HI, "Calculation of induced current densities and specific absorption rates (SAR) for pregnant women exposed to hand-held metal detectors," *Phys. Med. Biol.*, vol. 48, pp. 2551-2560, 2003.
- [9] Chengyu S, George X, "Development of a 30-week-pregnant female tomographic model from computed tomography (CT) images for Monte Carlo organ dose calculations," *Med. Phys.*, vol. 31, 2491-2497
- [10] Sederberg TW, Parry SR, "Free-form Deformation of Solid Geometric Models," *ACM Siggraph Conference Proceedings*, 1986.
- [11] Zentani Y, Yamana N, "Studies on the maternity robes", *The journal of clothing of Kyoto Woman's University*, vol. 25, pp. 16-22, 1980. (In Japanese)
- [12] Araki T, "Obstetrics for the new millennium-normal pregnant women-," Tokyo, Bunkodo, 2001.
- [13] Ramsay MM, James DK, Weiner CP, Gonik B, "Normal values in pregnancy, second edition", Philadelphia, WB Saunders, 2000.
- [14] ICNIRP, "Guidelines for limiting exposure to time-varying electric, magnetic, and electromagnetic fields (0 Hz to 300 GHz)," *Health Phys.*, vol. 74, no. 4, pp. 494-522, Apr. 1998.
- [15] Berenger JP, "A perfectly matched layer for the absorption of electromagnetic waves," *Journal of computational physics*, pp. 185-200, 1994.
- [16] Gabriel C, "Compilation of the dielectric properties of body tissues at RF and microwave frequencies," *Armstrong Laboratory, Brooks Air Force Base, Tech. Rep. AL/OE-TR-1996-0037*, 1996.
- [17] Gabriel C, Gabriel S, Corthout E, "The dielectric properties of biological tissues: I. Literature survey," *Phys. Med. Biol.*, vol. 41, pp. 2231-2249, 1996.
- [18] Gabriel S, Lau RW, Gabriel C, "The dielectric properties of biological tissues: II. Measurements in the frequency range 10 Hz to 20 GHz," *Phys. Med. Biol.*, vol. 41, pp. 2251-2269, 1996.
- [19] Gabriel S, Lau RW, Gabriel C, "The dielectric properties of biological tissues: III. Parametric models for the dielectric spectrum of tissues," *Phys. Med. Biol.*, vol. 41, pp. 2271-2293, 1996.